1-1-2020

The pancreas-specific form of secretory pathway calcium ATPase 2 regulates multiple pathways involved in calcium homeostasis

Melissa Fenech

McKenzie M Carter

Peter B Stathopulos

Christopher Pin

BBA - Molecular Cell Research 1867 (2020) 118567

Contents lists available at ScienceDirect

BBA - Molecular Cell Research

journal homepage: www.elsevier.com/locate/bbamcr

The pancreas-specific form of secretory pathway calcium ATPase 2 regulates multiple pathways involved in calcium homeostasis

Melissa A. Fenech[a,d], McKenzie M. Carter[a,d], Peter B. Stathopulos[a], Christopher L. Pin[a,b,c,d,*]

[a] Department of Paediatrics, Schulich School of Medicine & Dentistry, University of Western Ontario, Canada
[b] Department of Physiology and Pharmacology, Schulich School of Medicine & Dentistry, University of Western Ontario, Canada
[c] Department of Oncology, Schulich School of Medicine & Dentistry, University of Western Ontario, Canada
[d] Children's Health Research Institute, London, ON, Canada

ARTICLE INFO

Keywords:
Secretory pathway calcium ATPase 2
Orai1
Store operated calcium entry
Store independent calcium entry
STIM1
Calcium signaling

ABSTRACT

Acinar cell exocytosis requires spatiotemporal Ca^{2+} signals regulated through endoplasmic reticulum (ER) stores, Ca^{2+}ATPases, and store-operated Ca^{2+} entry (SOCE). The secretory pathway Ca^{2+}ATPase 2 (SPCA2) interacts with Orai1, which is involved in SOCE and store independent Ca^{2+} entry (SICE). However, in the pancreas, only a C-terminally truncated form of SPCA2 (termed SPAC2C) exists. The goal of this study was to determine if SPCA2C effects Ca^{2+} homeostasis in a similar fashion to the full-length SPCA2.

Using epitope-tagged SPCA2C ($SPCA2C^{FLAG}$) expressed in HEK293A cells and Fura2 imaging, cytosolic [Ca^{2+}] was examined during SICE, SOCE and secretagogue-stimulated signaling. Exogenous SPCA2C expression increased resting cytosolic [Ca^{2+}], Ca^{2+} release in response to carbachol, ER Ca^{2+} stores, and store-mediated and independent Ca^{2+} influx. Co-IP detected Orai1-SPCA2C interaction, which was altered by co-expression of STIM1. Importantly, SPCA2C's effects on store-mediated Ca^{2+} entry were independent of Orai1. These findings indicate SPCA2C influences Ca^{2+} homeostasis through multiple mechanisms, some of which are independent of Orai1, suggesting novel and possibly cell-specific Ca^{2+} regulation.

1. Introduction

Cellular calcium (Ca^{2+}) is a critical second messenger required for cellular processes involved in cell function, survival and apoptosis [1–3]. Cytosolic Ca^{2+} levels need to be tightly regulated both temporally and spatially as constitutively high levels of cytosolic Ca^{2+} are detrimental to the cell. Therefore, several mechanisms are in place to keep sources of Ca^{2+} available yet sequester Ca^{2+} away from the cytosol, thereby allowing transient Ca^{2+} increases when required.

Proper Ca^{2+} signaling is particularly critical for regulated exocytosis in pancreatic acinar cells. At rest, Ca^{2+}ATPases, buffering proteins and Ca^{2+} channels all work to maintain low cytosolic Ca^{2+} (~100 nM) relative to the endoplasmic reticulum (ER) lumen (~0.4–0.7 mM) and extracellular space (~1 mM) [4–6]. Exocytosis is stimulated by secretagogues binding to cell surface receptors leading to activation of the inositol 1,4,5-trisphosphate (IP_3) pathway and promotion of Ca^{2+} transients in the apical pole of the cell [7–10]. IP_3 receptors (IP_3R) and ryanodine receptors (RyR) on the ER facilitate Ca^{2+} efflux from the ER, while plasma membrane Ca^{2+}ATPases (PMCA) and sarco/endoplasmic reticulum Ca^{2+}ATPases (SERCA) quickly clear Ca^{2+} from the cytosol. The combination of IP_3R/RyR and ATPase activity promotes oscillatory Ca^{2+} signals critical for enzyme exocytosis [11,12]. As Ca^{2+} is steadily removed from the ER and shuttled out of the cytoplasm by PMCAs, there is a net loss of Ca^{2+} stores in the ER. The depletion of Ca^{2+} within the ER triggers store operated Ca^{2+} entry (SOCE). ER Ca^{2+} is monitored by stromal interaction molecule 1 (STIM1), which senses Ca^{2+} through an EF-hand domain that resides in the ER lumen. When ER Ca^{2+} concentrations decrease, STIM1 undergoes a conformational change involving oligomerization and translocation to ER/PM junctions, where it activates Orai1 allowing extracellular Ca^{2+} influx into

Abbreviations: Co-IP, Co-immunoprecipitation; EGFP, Enhanced Green Fluorescent Protein; ER, Endoplasmic Reticulum; GPCR, G-protein coupled receptor; HBSS, Hanks balanced salt solution; HEK293A, Human embryonic kidney cells; $HEK\text{-}Orai1^{YFP}$, Human embryonic kidney cells expressing a fusion Orai1-YFP protein; IP_3, Inositol 1,4,5-trisphosphate; IP_3R, Inositol 1,4,5-trisphosphate Receptor; NFAT, Nuclear Factor of Activated T Cell; PMCA, Plasma membrane Ca^{2+} ATPase; RyR, Ryanodine receptor; SERCA, Sarcoendoplasmic reticulum Ca^{2+} ATPase; SOCE, Store operated Ca^{2+} entry; SPCA2, Secretory Pathway Ca^{2+} ATPase 2; SICE, Store independent Ca^{2+} entry; STIM1, Stromal interaction molecule 1; TG, Thapsigargin

* Corresponding author at: Dept. of Paediatrics, University of Western Ontario, Children's Health Research Institute, 5th Floor, Victoria Research Laboratories, London, Ontario N6C 2V5, Canada.
E-mail address: cpin@uwo.ca (C.L. Pin).

https://doi.org/10.1016/j.bbamcr.2019.118567
Received 10 July 2019; Received in revised form 7 October 2019; Accepted 8 October 2019
Available online 30 October 2019
0167-4889/

the cytosol for refilling of ER stores [13–15]. Additional studies indicate Orai1 also contributes to Ca^{2+} release-activated channels (CRAC) and is required for SOCE [16].

Orai1 also directly interacts with secretory pathway Ca^{2+} ATPase 2 (SPCA2), a member of a third family of Ca^{2+} ATPases. The SPCA2-Orai1 interaction occurs independent of ER Ca^{2+} store depletion, constitutively acting to increase cytosolic Ca^{2+} levels. This pathways has been termed store independent Ca^{2+} entry (SICE), and increased SPCA2 expression correlates with increases in cytosolic Ca^{2+} concentrations [17]. This represents a unique dual function for SPCA proteins, as they may utilize their Ca^{2+} ATPase function to promote Ca^{2+} uptake into the Golgi apparatus or promote SICE independent of primary active transport.

Assessment of SPCA2C's role in Ca^{2+} homeostasis has been limited but its expression pattern suggests unique functions in the pancreas. Our previous studies showed only a truncated form of SPCA2 (termed SPCA2C) is expressed within pancreatic acinar cells. SPCA2C is transcribed from an alternative start site that includes only the last four exons of the SPCA2 coding sequence, thereby eliminating domains required for SPCA2 to function as a Ca^{2+} ATPase [18]. Acinar cells are highly sensitive to altered Ca^{2+} homeostasis. Improper Ca^{2+} signaling and regulation disrupts exocytosis and promotes cellular damage associated with pancreatitis [2,3]. Inhibition of Orai1 or Ca^{2+} influx mediated by other channels decreased the severity of pancreatitis [19], and decreased accumulation of SPCA2C is observed following initiation of secretagogue-induced pancreatitis [18]. Since SPCA2C is the only isoform expressed in the pancreas, it is important to determine its involvement in store-operated or store-independent Ca^{2+} entry, Ca^{2+} signaling and Ca^{2+} homeostasis.

The goal of this study was to determine if SPCA2C maintains the non-traditional roles exhibited by the full length SPCA2 in the context of Ca^{2+} movement. In HEK 293A cells, SPCA2C expression localized to the ER and increased ER Ca^{2+} stores and Ca^{2+} influx after ER store depletion. Using HEK293A cells with and without stable expression of Orai1, we determined that SPCA2C interacts with Orai1 to mediate SICE. Importantly, this role in Ca^{2+} influx upon store depletion was independent of Orai1, suggesting a novel mechanism for regulating Ca^{2+} influx.

2. Methods

2.1. Protein sequence comparison

The NCBI reference codes for the *Xenopus tropicalis* (frog), *Notechis scutatus* (snake), *Mus musculus* (mouse), *Homo sapiens* (human), *Sus scrofa* (pig), *Bos taurus* (cow) and *Felis catus* (cat) amino acid sequences used in the alignment are NP 001072524.1, XP 026539825.1, NP_081198.1, NP_055676.3, XP_003126874.1, XP_002694791.2 and XP 023101802.1, respectively. The sequence alignment was performed using Clutal Omega [20] and PSIPRED [21] used for predicting structure.

2.2. Plasmid construction

A *pcDNA3.1-SPCA2C^{FLAG}* expression vector was generated by GeneArt using the mouse *Atp2c2* sequence (NCBI accession #:AC_000030.1). A FLAG antigenic tag sequence

(5′ GATTACAAGGATGACGACGATAAG 3′) was placed in frame at the 3′ end of the *Atp2c2* coding sequence. *pcDNA3.1-SPCA2C^{mRFP}* was generated by inserting PCR-amplified *Atp2c2c* into the *XhoI* and *BamHI* sites, using forward primer sequence

3′ CTAGGCGGCCGCGCTCCACGGACT 5′ and reverse primer sequence

3′ CTAGCTCGAGCACAGCTTCC 5′ in *pcDNA3.1-mRFP*. *pcDNA3.1-mRFP* was a gift from Doug Golenbock (Addgene plasmid # 13032; http://n2t.net/addgene:13032; RRID:Addgene_13032). All plasmid sequences were verified by the London Regional Genomics Centre (Western University, London, ON).

2.3. Cell culture

Human embryonic kidney (HEK) 293A cells were maintained in Dulbecco's Modified Eagle Medium (DMEM) with 4.5 g/L D-glucose, L-Glutamine containing 10% FBS and 1% Penstrep. HEK293A cells stably expressing YFP-tagged Orai1 (HEK-Orai1^{YFP}) were a generous gift from Dr. Monica Vig (Tata Institute of Fundamental Research, India) [22]. HEK-Orai1^{YFP} cells were maintained in DMEM with 4.5 g/L L-glutamine and sodium pyruvate; containing 10% FBS, 1% Penstrep and 4 mg/mL G418. When cultures reached 70–80% confluence, cells were transfected using JetPrime transfection kit (Polyplus, NY), with *pcDNA3.1-SPCA2C^{FLAG}*, *pcDNA3.1-SPCA2^{MYC}* (encodes full length SPCA2; kindly provided by R. Rao) [17] or *pCMV6-Stim1^{mCherry}*, which encodes a monomeric cherry fluorescence protein fused to the N-terminus of STIM1, immediately downstream of the ER signal peptide [23,24].

For Nuclear Factor of Activated T cell (NFAT) experiments, HEK293A cells were transfected using JetPrime system (Polyplus Transfection, New York, NY, USA; cat#114-07) with *pCORON1000-NFAT-EGFP* and *pcDNA3.1-Atp2c2c^{mRFP}* or *pcDNA3.1-Atp2c2^{MYC}*. Cells were incubated in transfection mixture for 24 h before analysis. As a control, HEK293A cells transfected with *pCORON1000-NFAT-EGFP* only were treated with 2 μM TG in 2 mM Ca^{2+} for 30 min at 37 °C and 5% CO_2, then fixed with 4% formalin.

2.4. Calcium imaging

48 h after transfection, HEK-Orai1^{YFP} +/- *pcDNA3.0-GFP* and/or *pcDNA3.1-SPCA2C^{FLAG}*, or *pcDNA3.1-SPCA2^{MYC}*, cells were loaded with Fura-2 AM at 1–3 μM in culture media for 30 min at 37 °C and 5% CO_2. After loading, cells were rinsed once in Hank's Buffered Saline Solution (HBSS) supplemented with 1.8 mM Ca^{2+} (unless otherwise stated) and allowed to equilibrate to 37 °C. Fura2 emission was measured as previously described [18] in individual cells. To examine SPCA2C's effects on Ca^{2+} release in response to GPCR signaling, individual groups of cells were stimulated with 10 μM carbachol for 5 min at a pressure of 2 Pa by puffing. Five-minute puffing experiments were completed no more than three times per plate, and never on the same group of cells. To examine SOCE and intracellular Ca^{2+} stores, cells were treated with 2 μM thapsagargin and 2 mM EGTA followed by either ionomycin (1 μM) or Ca^{2+} (2 mM, 4 mM, 6 mM) addition back to HBSS media. To examine SICE, cells were loaded with Fura-2 as described above and a resting level of cytosolic Ca^{2+} achieved in 0 mM Ca^{2+} HBSS, Ca^{2+} was added to the media in incremental amounts (1.0 mM or 2.0 mM Ca^{2+}) and intracellular Ca^{2+} recorded for 3 min. Ca^{2+} influx rate was calculated as:

$$R^{\Delta}{}_{340/380} = (\underline{R^{F}}_{340/380} - \underline{R^{I}}_{340/380})/60$$

where R^F is the final 340/380 ratio, which were normalized to R^I values, R^I represents the initial 340/380 ratio and 60 is the time in seconds for recording after Ca^{2+} was added to media. N values are provided within the figure legends for each experiment. Data is shown as the mean ± SE and significance determined using two-way ANOVA and Sidak's or Tukey's posthoc test.

2.5. Protein collection, Western blotting and co-immunoprecipitation

Cells were transfected as described with 5 μg of *pcDNA3.1-SPCA2C^{FLAG}* +/- 0–5 μg of *pCMV6-Stim1^{mCherry}*. Cells were harvested by trypsinization 72 h after transfection, washed with cold PBS, and incubated in a mild lysis buffer (150 mM NaCl, 50 nM HEPES pH 7.4, 25 μg/mL digitonin [SIGMA; cat.#D141]) for 10 min. Samples were

centrifuged at 2000 RCF, and supernatant collected for the cytosolic protein fraction. The remaining insoluble pellet was washed with PBS, resuspended in a second lysis buffer (150 mM NaCl, 50 nM HEPES pH 7.4, 1% NP40), and incubated 40 min with mild agitation. Samples were centrifuged at 7000 RCF for 10 min, and supernatant used as the membrane protein fraction.

All antibodies, sources and dilutions are listed in Supplementary Table S1. Western Blot analysis was performed as described [25]. Briefly, 15–60 μg of protein was separated by SDS-PAGE and transferred to polyvinylidene diflouride (PVDF) membrane (BioRad, Hercules, CA). Following a 1-hour incubation in blocking solution (5% non-fat skim milk in tris-buffered saline and 0.1% Tween 20 [TBST]), membranes were incubated in 1° antibodies diluted in TBS overnight at 4 °C. Following several washes with TBS, membranes were incubated in 2° antibodies diluted in TBS for 1 h at room temperature. Protein expression was visualized using Bio-Rad Clarity Western ECL substrate on a Bio-Rad VersaDoc Imaging System (BioRad; Hercules, CA).

For co-immunoprecipitation (co-IP) experiments, 400 μg of protein from HEK293A or HEK-Orai1^{YFP} cells transfected with SPCA2C +/- STIM1 were incubated with G-Sepharose beads (Invitrogen Dynabeads) and Orai1 antibody (Sigma) overnight at 4 °C. Samples were washed 4× in second lysis buffer. IP samples were resolved by SDS-PAGE and transferred to PVDF membrane. Western blotting was performed as described above.

2.6. Immunofluorescence analysis

HEK293A cells were transfected as described above with *pcDNA3.1-SPCA2C^{FLAG}* and/or *pcDNA3.1-STIM1^{mCherry}*. Forty-eight hours after transfection, HEK293A cells were fixed with 4% formaldehyde in PBS. IF was performed as described (Garside et al., 2010). All antibodies used (Supplemental Table S1) were diluted in blocking solution (PBS, 5% BSA, 1% Triton). Fluorescently labelled secondary goat antibodies were diluted 1:250 in PBS (Jackson Immunoresearch Labs, West Grove, PA or Sigma, Oakville, ON, Canada). Images acquired using Leica TCS SP5 II microscope. For NFAT experiments, formalin-fixed cells were stained with DAPI for 5 min and then visualized for RFP (SPCA2C) or EGFP (NFAT). IF was performed on cells transfected with *pcDNA-Atp2c2^{MYC}* as above using a rabbit α-MYC primary (1:500; SIGMA) and TRITC-conjugated α-rabbit IgG (1250).

3. Results

Since SPCA2C is the predominant isoform expressed in pancreatic acinar cells, we first investigated whether it served similar functions to the full length SPCA2. Previous work showed SPCA2 interacts with Orai1 to enhance store independent Ca^{2+} entry (SICE) through its C-terminal domain [17], which is identical to SPCA2C. To determine if this C-terminal domain function was conserved among phylogeny, we performed in silico analysis comparing the C-terminal domain of SPCA2 from different species. At least 8 polar and non-polar residue positions within the 20 residue C-terminal domain, which is downstream of the final transmembrane helix, are fully or partially conserved among different species (Fig. 1A) suggesting that the function of the C-terminal domain is likely retained and important in higher and lower vertebrates. Additionally, PSIPRED [26] analysis indicated that this C-terminal region of SPCA2 has a propensity to form an α-helix (Fig. 1A). It is noteworthy that intermolecular α-helix interactions between STIM1 and Orai1 underlie Orai1 channel assembly and gating in SOCE [27,28].

Given our bioinformatics analysis suggesting the C-terminal domain of SPCA2 may form a structural motif conducive to activation of Orai1 channels, we assessed whether SPCA2C interacts with Orai1. To determine if SPCA2C directly interacted with Orai1, co-IP was performed on membrane-enriched protein fractions following SPCA2C^{FLAG} transfection into HEK293A cells, which do not express Orai1, or HEK 293A cells stably expressing an Orai1- YFP fusion protein (HEK-Orai1^{YFP}). IF indicated SPCA2C^{FLAG} accumulates throughout HEK-Orai1^{YFP} cells with some overlap with Orai1 (Fig. 1B). Co-IP showed SPCA2C is readily pulled down by Orai1 IP (Fig. 1C). Remarkably, co-expression of STIM1 competed away the SPCA2C-Orai1 interaction and reduced accumulation of SPCA2C^{FLAG} in the membrane only when Orai1 was present (Fig. 1C). IF for SPCA2C^{FLAG} +/- STIM1 protein supported the finding that STIM1 affected SPCA2C membrane localization. Without STIM1, SPCA2C showed co-localization with Orai1 (Fig. 1D). The cellular localization of SPCA2C^{FLAG} also became more diffuse and did not overlap with Orai1 when STIM1^{mCherry} was present. Therefore, SPCA2C appears to bind Orai1 through a similar region as STIM1.

We next examined the ability for SPCA2C to increase resting cytosolic Ca^{2+}. Epitope-tagged versions of full length SPCA2 (SPCA2^{MYC}) or SPCA2C (SPCA2C^{FLAG}) were expressed in HEK-Orai1^{YFP} cells. Similar to HEK293A cells, HEK-Orai1^{YFP} cells do not normally express SPCA2 or SPCA2C (data not shown). Examination of cytosolic Ca^{2+} levels, in 1.8 mM extracellular Ca^{2+}, using Fura2 ratiometric imaging showed both SPCA2^{MYC} ($R_{340/380} = 0.43 \pm 0.02$) and SPCA2C^{FLAG} ($R_{340/380} = 0.58 \pm 0.03$) significantly increased resting cytosolic Ca^{2+} concentrations in HEK-Orai1^{YFP} cells compared to GFP alone ($R_{340/380} = 0.26 \pm 0.01$; Fig. 1E). The increase in cytosolic Ca^{2+} levels in HEK-Orai1^{YFP} cells was also significantly higher when comparing cells expressing SPCA2C^{FLAG} to SPCA2^{MYC} ($p < 0.05$; Fig. 1E), suggesting SPCA2C may affect additional pathways involved in Ca^{2+} homeostasis that SPCA2 does not.

To determine if the ability of SPCA2C to increase cytosolic Ca^{2+} was due to an increased rate of Ca^{2+} influx across the plasma membrane through SICE, GFP was expressed +/- SPCA2C in HEK- Orai1^{YFP} cells and incubated in nominally Ca^{2+}-free media followed by addition of Ca^{2+} back to the media. Incremental addition of Ca^{2+} to the media resulted in a significant increase in the rate of Ca^{2+} influx in SPCA2C-expressing cells compared to GFP-only expressing cells. At 1 mM Ca^{2+}, SPCA2C-expressing cells showed a 2.7-fold increase in Ca^{2+} influx ($^{\Delta}R_{(340/380)}/sec = 3.95 \times 10^{-4} \pm 6.79 \times 10^{-5}$) vs. GFP-expressing cells ($^{\Delta}R_{(340/380)}/sec = 1.48 \times 10^{-4} \pm 4.11 \times 10^{-5}$). At 2 mM extracellular Ca^{2+}, Ca^{2+} influx was still almost 2-fold higher in SPCA2C ($^{\Delta}R_{(340/380)}/sec = 5.95 \times 10^{-4} \pm 8.5 \times 10^{-5}$)vs. GFP-expressing cells ($^{\Delta}R_{(340/380)}/sec = 3.57 \times 10^{-4} \pm 7.03 \times 10^{-5}$) (Fig. 1F). These results suggest that SPCA2C enhances Ca^{2+} uptake into the cell through SICE.

IF showed SPCA2C is not only co-localized with Orai1 but also has an extensive pattern of expression throughout the cell. We previously showed SPCA2C has a different subcellular expression pattern than full length SPCA2 [18,29] suggesting diverse roles for SPCA2C in affecting Ca^{2+} homeostasis. To determine the subcellular localization of SPCA2C, HEK293A cells were transfected with *pcDNA3.1-SPCA2C^{mRFP}* and IF performed for organelle-specific markers (Fig. 2). We chose to determine SPCA2C cellular localization in HEK293A cells since the Orai1^{YFP} limited fluorochrome analysis. Co-localization of SPCA2C^{mRFP} with markers for the ER (Fig. 2A; Selenoprotein S) and Golgi (Fig. 2B; GM130) was readily observed. More than 75% of cells expressing SPCA2C^{mRFP} showed partial, if not complete, overlap with ER localized markers, while 50% of the cells showed complete or partial Golgi marker co-localization, indicating the expression pattern was not simply due to over-expression. Quantitative co-localization analysis was not reliable as IF images showed SPCA2C^{mRFP} localization is not limited specifically to the ER or Golgi. Conversely, limited localization of SPCA2C^{mRFP} was observed at the plasma membrane (Fig. 2C; E-catenin).

The localization of SPCA2C to the ER suggests it affects Ca^{2+} stores and Ca^{2+} release from this organelle. To examine ER Ca^{2+}, HEK-Orai1^{YFP} cells expressing GFP +/- SPCA2C were incubated in 1.8 mM extracellular Ca^{2+} then treated with thapsigargin (TG), which inhibits SERCA pumps, thereby promoting emptying of ER-associated Ca^{2+} stores [30]. ER Ca^{2+} levels were assessed by monitoring the transient

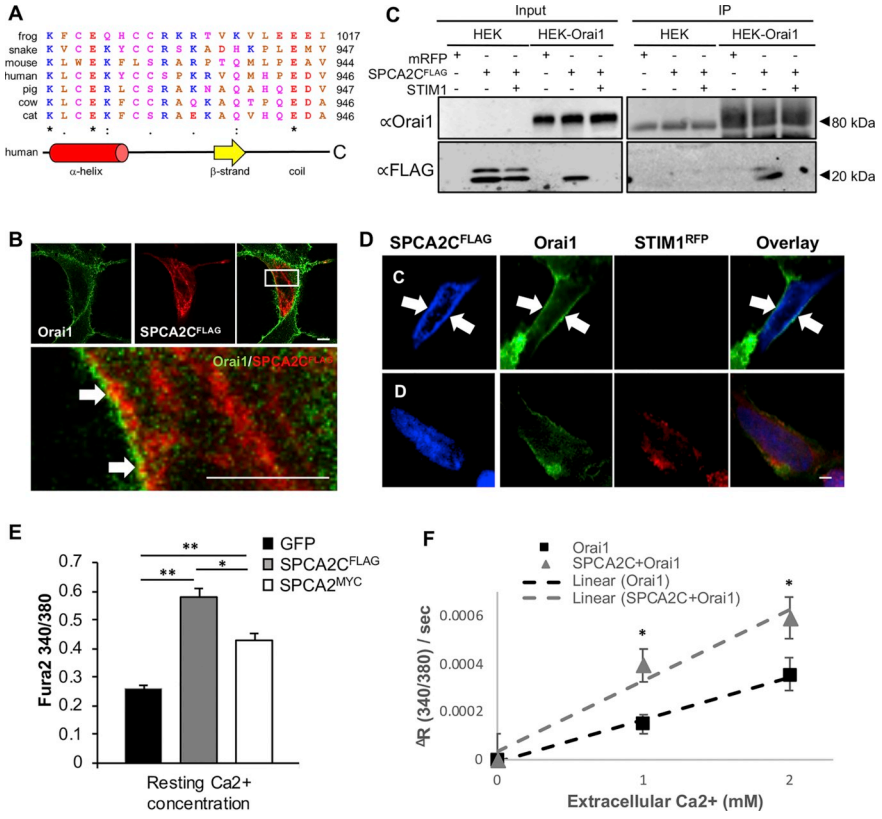

Fig. 1. SPCA2C interacts with Orai1 and increases cytosolic Ca^{2+} levels. (A) Sequence alignment of the C-terminal domain of SPCA2 in higher to lower vertebrates. Basic (blue), acidic (red), non-polar (brown) and polar residues (magenta) are identified. Completely (*), highly (:) and partially (.) conserved residues are indicated below the residue position. The C-terminal residue number of each sequence is shown at right. The PSPIRE predicted secondary structure composition of the human SPCA2 C-terminal domains is indicated below alignment. C, carboxy terminus. (B) IF for $SPCA2C^{FLAG}$ following transfection of HEK 293-$Orai1^{YFP}$ with SPCA2C (arrow). Scale bar = 5 μm. (C) Co-IP for Orai1 in HEK293A or HEK-$Orai1^{YFP}$ cells expressing mRFP or $SPCA2C^{FLAG}$ +/- $STIM1^{mCherry}$. Western blot for Orai1 or SPCA2C (FLAG) in membrane-enriched fractions (left panels) or following IP for Orai1 (right panels). Black arrow indicates Orai1; other bands reflect IgG. (D) IF for $SPCA2C^{FLAG}$ in HEK 293-$Orai1^{YFP}$ cells +/- $STIM1^{mCherry}$. Arrows indicate co-localization of Orai1 and SPCA2C. Scale bar = 5 μm. (E) Resting cytosolic Ca^{2+} levels recorded in HEK-$Orai1^{YFP}$ cells expressing SPCA2 (n = 15), SPCA2C (n = 13) or GFP only (n = 12). Cytosolic Ca^{2+} measurements were made using Fura2. Values expressed as mean ± SE; $^{*}p < 0.05$; $^{**}p < 0.01$. (F) Rates of Ca^{2+} influx in HEK293A cells expressing Orai1 (n = 22 [0 mM], 22 [1.0 mM], and 29 [2.0 mM]) or Orai1 + SPCA2 (n = 26 [0 mM Ca^{2+}], 22 [1.0 mM], and 32 [2.0 mM]).

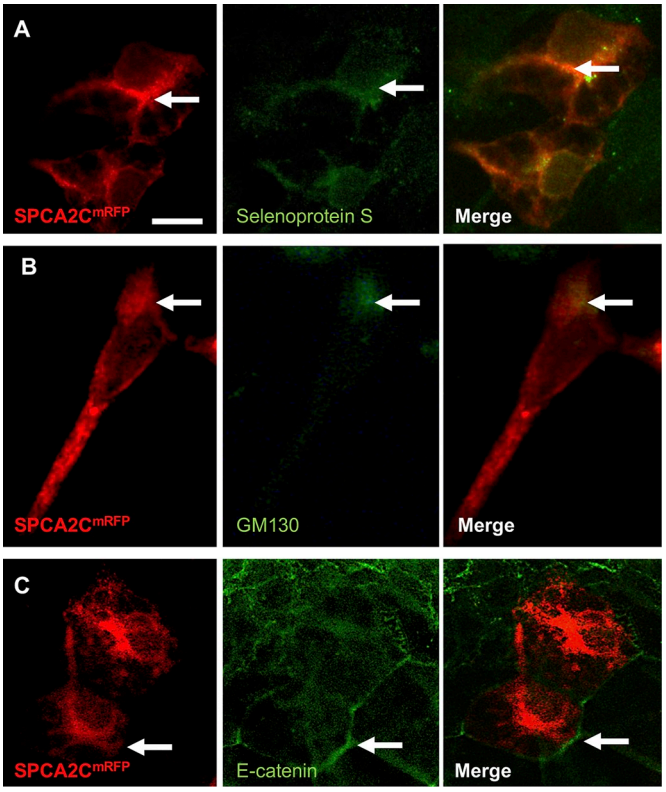

Fig. 2. SPCA2C protein localized to the endoplasmic reticulum and Golgi. Co-localization of $SPCA2C^{mRFP}$ ($SPCA2C^{mRFP}$; red) with Selenoprotien S (row A; green), GM130 (row B; green), or E-catenin (row C; green). Arrows indicate areas of co-localization. Scale bar = 10 μm.

increase in cytosol Ca^{2+} after TG treatment using Fura-2, as done previously [31,32]. Cells expressing SPCA2C showed a significant increase in cytosolic Ca^{2+} following TG treatment relative to GFP-expressing cells ($^{\Delta}R_{340/380}$ = 0.289 ± 0.013 vs. 0.139 ± 0.016; $p < 0.05$, Fig. 3A, B) suggesting SPCA2C increased Ca^{2+} levels in the ER. Subsequent treatment with ionomycin to empty all other Ca^{2+} stores showed no significant differences in cytosolic Ca^{2+} between GFP or SPCA2C-transfected cells ($^{\Delta}R_{340/380}$ = 0.063 ± 0.001 and 0.103 ± 0.001, respectively Fig. 3A, C) indicating increased Ca^{2+} levels following SPCA2C expression were specific to the ER. TG has been reported to also inhibit the full length SPCA2 [33], so it is possible the increases in cytosolic Ca^{2+} upon TG treatment are the result of ER and Golgi emptying of Ca^{2+}. Therefore, ER Ca^{2+} release was further tested by treating cells with carbachol, an acetylcholine receptor agonist that induces ER store-specific Ca^{2+} release through IP_3-mediated IP_3R activation. Cells were incubated in 1.8 mM extracellular Ca^{2+}, then treated with carbachol. In both SPCA2C and GFP expressing HEK-$Orai1^{YFP}$ cells, peak release of Ca^{2+} occurred rapidly upon carbachol stimulation (Fig. 3D). However, significantly more Ca^{2+} was released in response to carbachol in SPCA2C-expressing cells compared to GFP expressing HEK-$Orai1^{YFP}$ cells ($^{\Delta}R_{340/380}$ = 0.276 ± 0.04 vs. 0.080 ± 0.02, Fig. 3D, E). HEK-$Orai1^{YFP}$ cells expressing full length SPCA2 also showed significantly greater release in Ca^{2+} in response to carbachol relative to GFP-expressing cells ($^{\Delta}R_{340/380}$ = 0.226 ± 0.05 vs. 0.080 ± 0.02, Fig. 3E).

While increased ER Ca^{2+} levels in cells expressing SPCA2C could be due to enhanced Ca^{2+} uptake from the cytosol, SPCA2C does not contain the domains required for primary active Ca^{2+}ATPase activity capable of moving Ca^{2+} against the steep concentration gradient. Since SPCA2C localized to the ER, interacted with Orai1 and promoted increased ER Ca^{2+} stores, SPCA2C's effect on SOCE was examined. If SPCA2 is involved in SOCE, increased Ca^{2+} uptake and re-localization to interact with Orai1 should be observed upon Ca^{2+} store depletion. Using Fura2 ratiometric imaging, cytosolic Ca^{2+} influx was measured

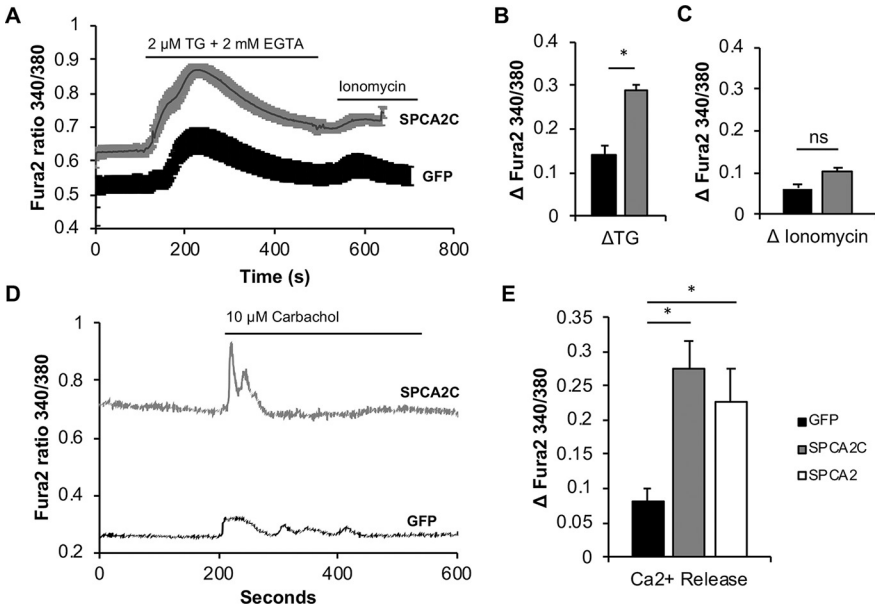

Fig. 3. SPCA2C increases ER Ca^{2+} stores in HEK-Orai1^{YFP} cells. (A) Ratiometric Fura2 analysis showing the response to thapsigargin (TG) or ionomycin treatment in HEK-Orai1^{YFP} cells expressing GFP ($n = 22$) or GFP + SPCA2C ($n = 23$). Maximal change in cytosolic Ca^{2+} based on Fura2 340/380 ratio in response to (B) TG or (C) ionomycin. Values expressed as mean ± SE; $^{*}p < 0.05$. (D) Ratiometric Fura2 traces showing response to carbachol stimulation in (HEK-Ora1^{YFP}) cells expressing GFP ($n = 8$) or GFP + SPCA2C^{FLAG} (n = 8). (E) Maximal change in cytosolic Ca^{2+} based on Fura2 340/380 ratio in response to carbachol in (HEK-Orai1^{YFP}) cells expressing GFP (n = 8) or GFP + SPCA2C^{FLAG} (n = 8), or GFP + SPCA2^{MYC} ($n = 6$). Values expressed as mean ± SE; $^{*}p < 0.05$.

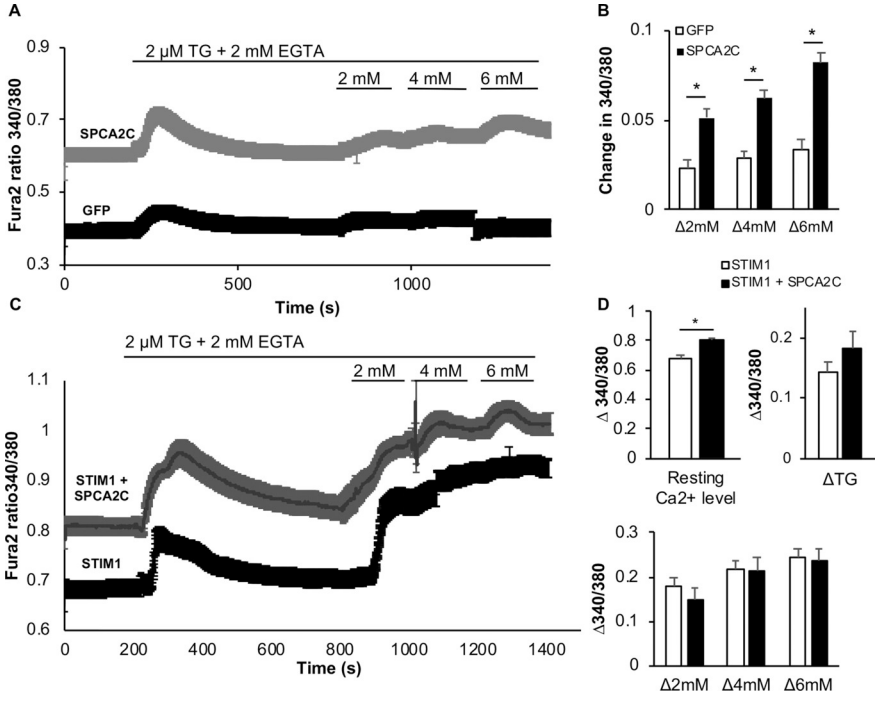

Fig. 4. SPCA2C increases cytosolic Ca^{2+} after store depletion. (A) Ratiometric Fura2 traces showing response to thapsigargin (TG) followed by increasing extracellular Ca^{2+} to the media in HEK-Orai1^{YFP} expressing GFP +/- SPCA2C, or (C) STIM1/GFP +/- SPCA2C. (B) Maximal changes in cytosolic Ca^{2+} following Ca^{2+} addback quantified for SPCA2C + GFP ($n = 33$) or GFP alone ($n = 28$). (C) Ratiometric Fura2 traces showing response to TG and Ca^{2+} addback in HEK-Orai1^{YFP} expressing STIM1/GFP +/-SPCA2C. (D) Quantification of resting Ca^{2+} levels, response to TG, and maximal change in cytosolic Ca^{2+} following Ca^{2+} addition quantified for SPCA2C + STIM1 + GFP ($n = 25$) or STIM1 + GFP (n = 33). Values expressed as mean ± SE; $^{*}p < 0.0001$.

in HEK-Orai1^{YFP} cells expressing GFP +/- SPCA2C during incremental add back of Ca^{2+} following store depletion with TG and EGTA. HEK-Orai1^{YFP} cells expressing SPCA2C showed significantly greater Ca^{2+} influx following addition of Ca^{2+} back to the media, compared to GFP-only expressing ($^{\Delta}R_{340/380}$ at 6 mM Ca^{2+} = 0.08 ± 0.005 vs. 0.03 ± 0.005; $p < 0.05$, Fig. 4A, B), indicating that SPCA2C influences Ca^{2+} influx rates after store depletion. Similar experiments with HEK-Orai1^{YFP} cells expressing SPCA2C + STIM1 resulted in significantly greater resting levels of cytosolic Ca^{2+} at rest compared to STIM1-only expressing cells ($R_{340/380}$ = 0.803 ± 0.027 vs. 0.683 ± 0.017; $p < 0.0001$, Fig. 4C, D). However, no further increase in ER Ca^{2+} release or SOCE occurred when STIM1 and SPCA2C were co-expressed ($^{\Delta}R_{340/380}$ at 6 mM Ca^{2+} = 0.24 ± 0.03 and 0.24 ± 0.02; respectively, Fig. 4D).

Next, we examined the localization of SPCA2C in response to ER Ca^{2+} store depletion. As observed previously (Fig. 1), some co-localization between SPCA2C and Orai1 was readily observed under resting Ca^{2+} levels (Fig. 5A). Upon TG treatment and concomitant chelation of extracellular Ca^{2+} using EGTA, no increase in SPCA2C-Orai1 co-localization occurred (Fig. 5B). Conversely, HEK-Orai1^{YFP} cells expressing STIM1 showed prominent Orai1-STIM1 puncta upon TG treatment, consistent with SOCE (Fig. 5C, D). When STIM1 and SPCA2C were co-expressed in HEK-Orai1^{YFP} cells and treated with TG, STIM1 and Orai1 again formed distinct foci that were largely devoid of SPAC2C accumulation (Fig. 5E, F).

These results suggest the ability of SPCA2C to increase ER Ca^{2+} and affect the response to ER store depletion may be independent of Orai1. Indeed, we previously showed SPCA2C increased cytosolic Ca^{2+} in HEK293A cells, which do not express Orai1 [18]. To determine if Orai1 is required for increased Ca^{2+} influx under resting condition or following ER Ca^{2+} store depletion, HEK293A cells were transfected with SPCA2C (Fig. 6). Fura2 imaging was used to assess Ca^{2+} uptake with

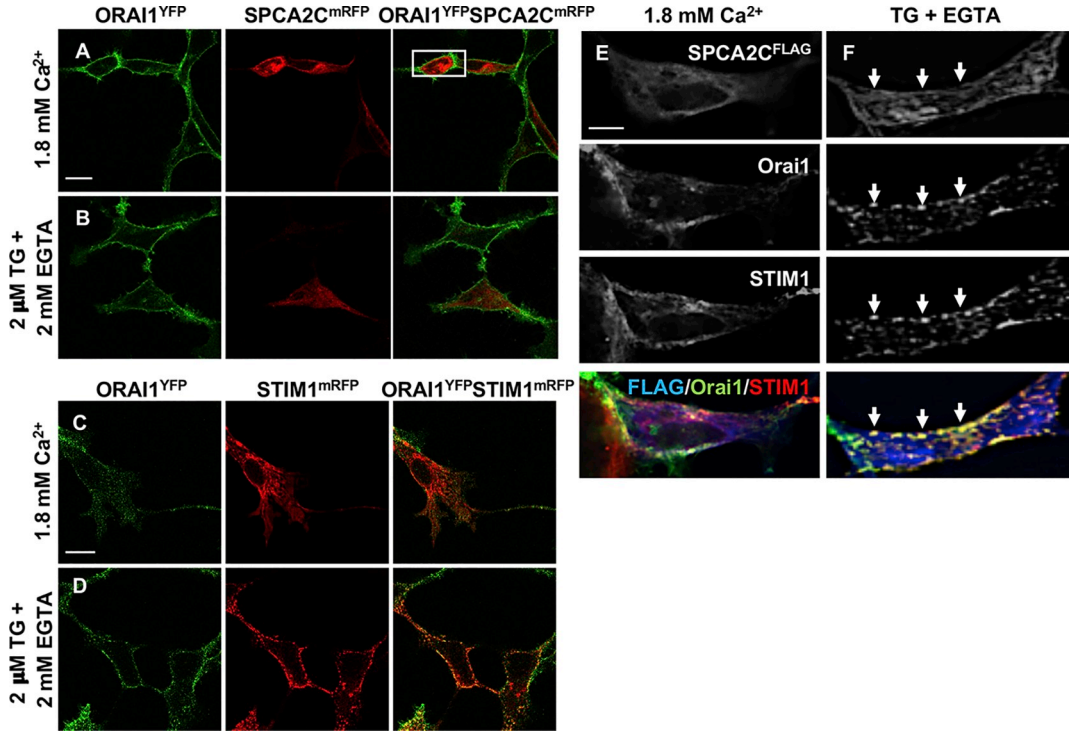

Fig. 5. SPCA2C localization in HEK-Orai1^{YFP} cells does not change when ER stores are depleted. Fluorescent localization of (A, B) SPCA2C^{mRFP} or (C, D) STIM1^{mCherry} in HEK-Orai1^{YFP} cells under (A, C) physiological Ca^{2+} conditions (1.8 mM Ca^{2+}) or (B, D) following thapsigargin (TG) treatment. STIM1^{mCherry} protein forms puncta co-localizing with Orai1^{YFP} (white arrow) following emptying of ER stores by treatment with 2 µM TG. Scale bar = 2.5 µm. Co-IF for STIM1^{mCherry} and SPCA2C^{FLAG} (E) under physiological Ca^{2+} conditions (1.8 mM Ca^{2+}) or (F) following TG treatment in HEK-Orai1^{YFP} cells expressing SPCA2C^{FLAG} and STIM1^{mCherry}. Scale bar = 2.5 µm.

the addition of extracellular Ca^{2+} independent of ER Ca^{2+} store depletion (i.e. SICE). HEK293A cells expressing SPCA2C showed no significant increases in Ca^{2+} influx rate with the addition of extracellular Ca^{2+} (Fig. 6A) suggesting the ability of SPCA2C to enhance SICE is dependent on the presence of Orai1. However, as observed in HEK-Orai1^{YFP} cells, Ca^{2+} release from ER stores after treatment with TG and EGTA was significantly higher in HEK293A cells expressing SPCA2C compared to cells expressing GFP only ($^{\Delta}R_{340/380}$ = 0.133 ± 0.018 vs. 0.036 ± 0.009; $p < 0.0001$, Fig. 6B, C), and treatment with ionomycin showed no difference in Ca^{2+} release from other organelles (Fig. 6D). Upon addition of Ca^{2+} back to the media after store depletion by TG and EGTA, Fura2 measurements showed HEK293A cells expressing SPCA2C had significantly increased Ca^{2+} influx ($^{\Delta}R_{340/380}$ at 6 mM = 0.070 ± 0.005 vs. 0.029 ± 0.002; $p < 0.001$, Fig. 6C, E), indicating SPCA2C increased Ca^{2+} influx across the plasma membrane, after store depletion, even in the absence of Orai1.

This data suggests SPCA2C functions to increase cytosolic Ca^{2+} in all situations. Previous studies indicated full length SPCA2's ability to increase cytosolic Ca^{2+} lead to increased NFAT localization [17]. To determine if the elevation of cytosolic Ca^{2+} signaling upon SPCA2C expression promotes a similar nuclear localization of NFAT, we co-transfected SPCA2C-mRFP and NFAT-EGFP into HEK293A cells and

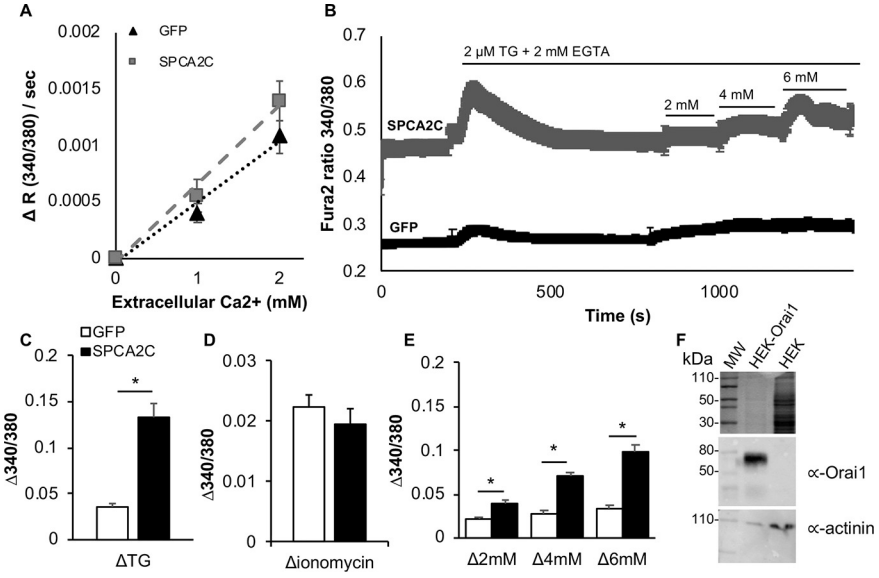

Fig. 6. SPCA2C increases Ca^{2+} entry during rest and after store depletion in the absence of Orai1. (A) Rate of Ca^{2+} influx in cells exposed to increasing extracellular Ca^{2+} (GFP: n = 29 [0 mM], 25 [1.0 mM], 34 [2.0 mM]; GFP + SPCA2: n = 29 [0 mM], 33 [1.0 mM], 30 [2.0 mM]). (B) Ratiometric Fura2 traces showing representative trace in response to TG and Ca^{2+} addback in HEK293A cells expressing GFP +/- SPCA2C. Maximal response to (C) TG, (D) ionomycin, or (E) increasing Ca^{2+}. *$p < 0.0001$. (F) Western blot showing no Orai1 expression in HEK293A cells. HEK293A cells expressing Orai1 have been included as a positive control, and western blotting for α-actinin provided as a loading control. Significantly more protein has been loaded for HEK293A cells to ensure no Orai1 expression is observed.

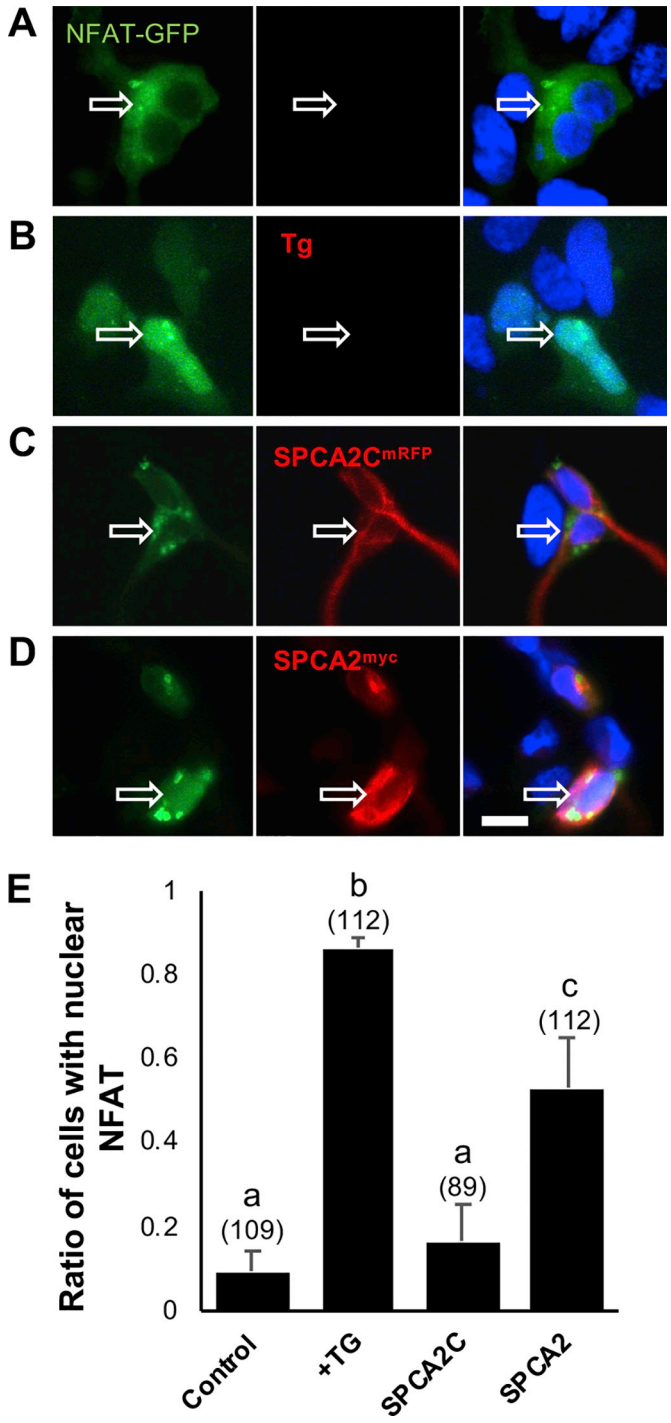

Fig. 7. SPCA2C expression does not enhance NFAT-EGFP nuclear localization in HEK293A cells. HEK293A cells with transfected with NFAT-EGFP alone (A) or in combination with SPCA2C^{mRFP} (C) or SPCA2^{MYC} (D) and localization assessed by fluorescent microscopy. As a positive control, NFAT-EGFP only-expressing cells were treated with TG (B). Arrows indicate individual nuclei of transfected cells. (E) Quantification of the percent of transfected cells with NFAT nuclear localization. Numbers in brackets indicate the total number of cells counted over three experiments. Letters indicate statistically different values. Error bars = mean ± SE. Magnification bar = 10 μm.

examined NFAT localization (Fig. 7). On its own, NFAT localized to the cytoplasm (Fig. 7A). As a control, we treated NFAT-EGFP-expressing cells with TG, which resulted in almost complete NFAT translocation (Fig. 7B). Interestingly, expression of SPCA2C did not enhance nuclear NFAT localization (Fig. 7C) suggesting the increase in cytosolic Ca^{2+} levels were not high enough to stimulation translocation. We performed similar experiments with a MYC-tagged full length SPCA2 (SPCA2^{MYC}; Fig. 7D). While nuclear localization was increased (Fig. 7E), translocation was often incomplete, maintaining partial NFAT-EGFP accumulation in the cytosol.

4. Discussion

Regulation of Ca^{2+} homeostasis is crucial for proper cell function, requiring several pathways to rapidly move Ca^{2+} into and out of the cytosol. One family of proteins involved in Ca^{2+} homeostasis is the secretory pathway Ca^{2+} ATPases, which consists of SPCA1 and SPCA2. Both SPCA proteins have been linked to Ca^{2+} homeostasis pathways not requiring ATPase function [34,35], however, it is unclear if these non-ATPase functions are regulated by other SPCA isoforms. In this study, we characterized the function of SPCA2C, the only isoform of SPCA2 expressed in pancreatic acinar cells [18]. SPCA2C contains the last four transmembrane domains of the full-length SPCA2 protein but lacks most of the domains required for Ca^{2+} ATPase activity. Our results indicated forced expression of SPCA2C increased Ca^{2+} influx in HEK293A cells through a store-independent mechanism dependent on Orai1, similar to full length SPCA2. However, SPCA2C also increased resting cytosolic Ca^{2+} concentrations, elevated Ca^{2+} levels in the ER, and promoted increased store-mediated Ca^{2+} influx, all independent of Orai1. These results suggest SPCA2C affects multiple pathways regulating cytosolic Ca^{2+} and does so through known and novel mechanisms.

SPCA2C readily interacts with Orai1 when expressed in HEK-Orai1^{YFP} cells. This is consistent with previous findings that showed only the C-terminal of SPCA2, which is maintained in SPCA2C, was required for Orai1 interaction [17]. The previous study also indicated that only C-terminal portions of SPCA2 elicited increased Ca^{2+} influx [17], confirming interactions between Orai1 and the C-terminal part of SPCA2 are functionally relevant on their own. Indeed, our results showed SPCA2C enhanced Orai1's ability to promote SICE. Unlike SPCA2, which localizes predominantly to the Golgi, we showed SPCA2C has a different localization pattern, accumulating also in the ER. This is consistent with studies that examined localization of C-terminal truncations of SPCA2 [36] and is also similar to the localization we previously documented in pancreatic acinar cells [29]. This difference in localization patterns between SPCA2 and SPCA2C may account for SPCA2C's ability to promote increased cytosolic Ca^{2+} levels relative to the full-length SPCA2 levels. We suggest full length SPCA2 would normally have limited interaction with Orai1 due to a lack of co-localization, and, therefore, different SPCA2 isoforms may be required for the different physiological roles related to Orai1and other Ca^{2+} influx channels. By localizing to the main Ca^{2+} storage department within the cell, SPCA2C has an increased opportunity to interact and effect Ca^{2+} levels throughout the cell.

The differential expression pattern may also account for differences in cell type-specific requirements for SICE. SPCA2C is the only SPCA2 isoform expressed to appreciable levels in acinar cells. SPCA2C's expression and ability to interact with Orai1 may indicate a greater physiological role for SICE in maintaining Ca^{2+} at appropriate levels, where ER Ca^{2+} stores are essential for enzyme exocytosis. Linking SPCA2C specifically to acinar cell physiology may also explain differences observed in NFAT localization following expression of SPCA2 or SPCA2C. While our analysis of SPCA2 did not result in complete NFAT nuclear localization, some was observed in the majority of cells. Conversely, SPCA2C did not increase NFAT nuclear localization even though cytosolic Ca^{2+} levels were increased. Previous studies linked SPCA2's ability to promote NFAT nuclear translocation in breast cancer and HEK293A cell lines [17], and SPCA2 is expressed to high levels in breast cancer cells lines suggesting it may be a pathological consequence of high SPCA2 levels. We are currently examining whether alterations in SPCA2C expression can affect acinar cell biology.

Despite its ability to interact with Orai1, SPCA2C's contribution to Orai1 function appears to be limited to SICE. Expressing SPCA2C increased cytosolic and ER Ca^{2+}, and increased influx of Ca^{2+} following ER-store depletion regardless of Orai1 expression. Previous studies examining full-length SPCA2 [17,35] and SPCA1 [35] ability to increase Ca^{2+} influx, indicated this occurred solely through SICE and specifically increased Golgi, but not ER Ca^{2+} stores [35,36]. SPCA2 expression did not affect ER stores, [17] while over-expression of SPCA1 promoted Golgi swelling and stress [35,36]. These results suggest that at least SPCA1 may have a pathophysiological role in SICE. Given SPCA2C's expression pattern in the pancreas, and its decreased expression following induction of injury, we suggest that SPCA2C, unlike SPCA1, has a unique physiological role in SICE.

It is tempting to suggest Orai1 interactions with SPCA2C and STIM1 reflect a switch from a normal physiological role to a stress-induced response. Co-expression of STIM1 and SPCA2C in HEK-$Orai1^{YFP}$ eliminated Orai1-SPCA2C interaction and disrupted the cellular localization of SPCA2C. Therefore, it appears STIM1 and SPCA2C bind Orai1 in similar regions. The α-helical secondary structure predicted for the C-terminal domain of SPCA2C is similar to the predominant secondary structure adopted by STIM1. Thus, SPCA2C binding with Orai1 may be mediated by intermolecular helix interactions as characterized for STIM1 and Orai1. This is consistent with previous findings that complexes containing Orai1 and SPAC2 do not contain STIM1 [17]. Also, we did not observe a change in STIM1-Orai1-mediated SOCE or localization when SPCA2C was expressed, however, SPCA2C localization was affected by the presence of STIM1, suggesting an interaction with Orai1 helps localize SPCA2C to the membrane. In confirmation of a role for Orai1 in SPCA2C localization, knock down of *Orai1* in SCp2 cells restricted SPCA2 localization to perinuclear region, with, less puncta near the membrane [34]. In addition, while SPCA2C promotes increases in Ca^{2+} uptake following store depletion, these increases are modest, and emptying of ER stores did not result in increased co-localization of Orai1 and SPCA2C. The re-localization of SPCA2C upon STIM1 expression does not appear to be strictly to the Golgi. Indeed, SPCA2C localization occurs throughout the cytoplasm and analysis of cytosolic fractions revealed a decrease in overall SPCA2C accumulation (data not shown) suggesting it is being degraded.

Surprisingly, membrane localization of SPCA2C was not disrupted by STIM1 in the absence of Orai1. Therefore, while Orai1 interactions may be required for membrane localization of SPCA2C, this requirement is only necessary when Orai1 is stably expressed. This seeming conundrum may be due to altered expression of proteins involved in Ca^{2+} influx when $Orai1^{YFP}$ is stably expressed. We and others have shown that HEK-$Orai1^{YFP}$ cells have reduced cytosolic Ca^{2+} compared to parental HEK293A cells, which is likely due to reduced expression of other channels that promote Ca^{2+} uptake. Therefore, STIM1 does not compete with proteins required for SPCA2C membrane localization in the absence of Orai1.

While we could not detect Orai1 protein in HEK293A cells, we cannot rule out potential interactions with other Orai proteins. No studies have examined Orai2 or Orai3 expression in HEK293A cells. However, cell-specific differences in the types of Ca^{2+} channels activated by ER Ca^{2+} store depletion have been documented, [37–39] and these different channels may interact with SPCA2C. For example, Transient receptor potential cation 1/3/6 (TRPC1/3/6) channels heavily influence SOCE [37–39]. Increased Ca^{2+} levels are associated with the initiation of pancreatitis and altering intracellular Ca^{2+} in the context of pancreatitis affects the progression and severity of acinar cell injury. Targeted deletion of the *Trpc3* gene or blocking Orai1 with a specific inhibitor significantly decreased SOCE in acinar cells and decreased the severity of experimental pancreatitis in mice [19,39]. Currently, clinical trials are underway using an Orai1 inhibitor in the treatment of pancreatitis. We showed a significant decrease in SPCA2C expression within 4 h of inducing experimental pancreatitis in mice suggesting SPCA2C function is perturbed in response to injury. In addition, we have observed a complete loss of SPCA2C in *Mist1*$^{-/-}$ mice, which have altered Ca^{2+} homeostasis, reduced exocytosis function, and an increased susceptibility to pancreatic disease.

In conclusion, this is the first evidence that SPCA2C affects multiple, non-ATPase related pathways that control Ca^{2+} homeostasis. Given SPCA2C is the predominant isoform expressed in pancreatic acinar cells, our work suggests that it plays an important physiological role in regulating Ca^{2+} within these cells. Whether decreased expression during injury is protective by reducing the potential for increased Ca^{2+} influx, or damaging, is unknown. Altering expression of SPCA2C in pancreatic acinar cells, as well as during experimentally induced pancreatitis, is currently being explored.

Supplementary data to this article can be found online at https://doi.org/10.1016/j.bbamcr.2019.118567.

Support

This work was supported by the Natural Sciences and Engineering Research Council [grant number 250225]. M. Fenech was supported by a University of Western Ontario Paediatrics scholarship, a Canada Graduate scholarship, and a studentship from the Natural Sciences and Engineering Research Council. M. Carter was supported by a University of Western Ontario Paediatrics summer scholarship.

CRediT authorship contribution statement

Melissa A. Fenech: Investigation, Methodology, Formal analysis, Writing - original draft, Writing - review & editing.**McKenzie M. Carter:**Investigation, Formal analysis.**Peter B. Stathopulos:** Methodology, Formal analysis, Writing - original draft, Writing - review & editing.**Christopher L. Pin:**Methodology, Formal analysis, Writing - original draft, Writing - review & editing, Funding acquisition.

Transparency document

The Transparency document associated with this article can be found, in online version.

Declaration of competing interest

The author(s) declare no competing interests.

References

[1] B. Kruger, E. Albrecht, M.M. Lerch, The role of intracellular calcium signaling in premature protease activation and the onset of pancreatitis, Am. J. Pathol. 157 (2000) 43–50, https://doi.org/10.1016/S0002-9440(10)64515-4.
[2] J. Li, R. Zhou, J. Zhang, Z.-F. Li, Calcium signaling of pancreatic acinar cells in the pathogenesis of pancreatitis, World J. Gastroenterol. 20 (2014) 16146–16152, https://doi.org/10.3748/wjg.v20.i43.16146.
[3] W. Zhou, F. Shen, J.E. Miller, Q. Han, M.S. Olson, Evidence for altered cellular calcium in the pathogenetic mechanism of acute pancreatitis in rats, J. Surg. Res. 60 (1996) 147–155, https://doi.org/10.1006/jsre.1996.0024.
[4] W.F. Pralong, C.B. Wollheim, R. Bruzzone, Measurement of cytosolic free Ca2+ in individual pancreatic acini, FEBS Lett. 242 (1988) 79–84.
[5] F.L. Bygrave, A. Benedetti, What is the concentration of calcium ions in the endoplasmic reticulum? Cell Calcium 19 (1996) 547–551.
[6] S. Hurwitz, Homeostatic control of plasma calcium concentration, Crit. Rev. Biochem. Mol. Biol. 31 (1996) 41–100, https://doi.org/10.3109/10409239609110575.
[7] E.A. Finch, T.J. Turner, S.M. Goldin, Calcium as a coagonist of inositol 1,4,5-trisphosphate-induced calcium release, Science. 252 (1991) 443–446.
[8] A. Futatsugi, T. Nakamura, M.K. Yamada, E. Ebisui, K. Nakamura, K. Uchida, T. Kitaguchi, H. Takahashi-Iwanaga, T. Noda, J. Aruga, K. Mikoshiba, IP3 receptor types 2 and 3 mediate exocrine secretion underlying energy metabolism, Science. 309 (2005) 2232–2234, https://doi.org/10.1126/science.1114110.
[9] I. Bezprozvanny, J. Watras, B.E. Ehrlich, Bell-shaped calcium-response curves of Ins(1,4,5)P3- and calcium-gated channels from endoplasmic reticulum of cerebellum, Nature. 351 (1991) 751–754, https://doi.org/10.1038/351751a0.
[10] S.V. Straub, D.R. Giovannucci, D.I. Yule, Calcium wave propagation in pancreatic acinar cells: functional interaction of inositol 1,4,5-trisphosphate receptors,

ryanodine receptors, and mitochondria, J. Gen. Physiol. 116 (2000) 547–560.
[11] A.V. Tepikin, S.G. Voronina, D.V. Gallacher, O.H. Petersen, Pulsatile Ca2+ extrusion from single pancreatic acinar cells during receptor-activated cytosolic Ca2+ spiking, J. Biol. Chem. 267 (1992) 14073–14076.
[12] B.C. Ponnappa, R.L. Dormer, J.A. Williams, Characterization of an ATP-dependent Ca2+ uptake system in mouse pancreatic microsomes, Am. J. Phys. 240 (1981) G122–G129, https://doi.org/10.1152/ajpgi.1981.240.2.G122.
[13] J. Roos, P.J. DiGregorio, A.V. Yeromin, K. Ohlsen, M. Lioudyno, S. Zhang, O. Safrina, J.A. Kozak, S.L. Wagner, M.D. Cahalan, G. Velicelebi, K.A. Stauderman, STIM1, an essential and conserved component of store-operated Ca2+ channel function, J. Cell Biol. 169 (2005) 435–445, https://doi.org/10.1083/jcb.200502019.
[14] J. Liou, M.L. Kim, W. Do Heo, J.T. Jones, J.W. Myers, J.E.J. Ferrell, T. Meyer, STIM is a Ca2+ sensor essential for Ca2+-store-depletion-triggered Ca2+ influx, Curr. Biol. 15 (2005) 1235–1241, https://doi.org/10.1016/j.cub.2005.05.055.
[15] M.M. Wu, J. Buchanan, R.M. Luik, R.S. Lewis, Ca2+ store depletion causes STIM1 to accumulate in ER regions closely associated with the plasma membrane, J. Cell Biol. 174 (2006) 803–813, https://doi.org/10.1083/jcb.200604014.
[16] M. Prakriya, S. Feske, Y. Gwack, S. Srikanth, A. Rao, P.G. Hogan, Orai1 is an essential pore subunit of the CRAC channel, Nature. 443 (2006) 230–233, https://doi.org/10.1038/nature05122.
[17] M. Feng, D.M. Grice, H.M. Faddy, N. Nguyen, S. Leitch, Y. Wang, S. Muend, P.A. Kenny, S. Sukumar, S.J. Roberts-Thomson, G.R. Monteith, R. Rao, Store-independent activation of Orai1 by SPCA2 in mammary tumors, Cell. 143 (2010) 84–98, https://doi.org/10.1016/j.cell.2010.08.040.
[18] M.A. Fenech, C.M. Sullivan, L.T. Ferreira, R. Mehmood, W.A. MacDonald, P.B. Stathopulos, C.L. Pin, Atp2c2 is transcribed from a unique transcriptional start site in mouse pancreatic Acinar cells, J. Cell. Physiol. 231 (2016) 2768–2778, https://doi.org/10.1002/jcp.25391.
[19] L. Wen, S. Voronina, M.A. Javed, M. Awais, P. Szatmary, D. Latawiec, M. Chvanov, D. Collier, J. Barrett, M. Begg, K. Stauderman, J. Roos, S. Grigoryev, S. Ramos, E. Rogers, J. Whitten, G. Velicelebi, M. Dunn, A.V. Tepikin, D.N. Criddle, R. Sutton, Inhibitors of ORAI1 prevent cytosolic calcium-associated injury of human pancreatic Acinar cells and acute pancreatitis in 3 mouse models, Gastroenterology 149 (2015) 481–492, https://doi.org/10.1053/j.gastro.2015.04.015.
[20] F. Sievers, A. Wilm, D. Dineen, T.J. Gibson, K. Karplus, W. Li, R. Lopez, H. McWilliam, M. Remmert, J. Soding, J.D. Thompson, D.G. Higgins, Fast, scalable generation of high-quality protein multiple sequence alignments using Clustal Omega, Mol. Syst. Biol. 7 (2011) 539, https://doi.org/10.1038/msb.2011.75.
[21] L.J. McGuffin, K. Bryson, D.T. Jones, The PSIPRED protein structure prediction server, Bioinformatics. 16 (2000) 404–405.
[22] Y. Miao, C. Miner, L. Zhang, P.I. Hanson, A. Dani, M. Vig, An essential and NSF independent role for alpha-SNAP in store-operated calcium entry, Elife. 2 (2013) e00802, , https://doi.org/10.7554/eLife.00802.
[23] R.M. Luik, M.M. Wu, J. Buchanan, R.S. Lewis, The elementary unit of store-operated Ca2+ entry: local activation of CRAC channels by STIM1 at ER-plasma membrane junctions., J. Cell Biol. 174 (2006) 815–825. doi:https://doi.org/10.1083/jcb.200604015.
[24] J. Zhu, X. Lu, Q. Feng, P.B. Stathopulos, A charge-sensing region in the stromal interaction molecule 1 luminal domain confers stabilization-mediated inhibition of SOCE in response to S-nitrosylation, J. Biol. Chem. 293 (2018) 8900–8911, https://doi.org/10.1074/jbc.RA117.000503.
[25] C.L. Johnson, J.Y. Weston, S.A. Chadi, E.N. Fazio, M.W. Huff, A. Kharitonenkov, A. Koester, C.L. Pin, Fibroblast growth factor 21 reduces the severity of cerulein-induced pancreatitis in mice, Gastroenterology. 137 (2009) 1795–1804, https://doi.org/10.1053/j.gastro.2009.07.064.
[26] D.T. Jones, Protein secondary structure prediction based on position-specific scoring matrices, J. Mol. Biol. 292 (1999) 195–202, https://doi.org/10.1006/jmbi.1999.3091.
[27] X. Yang, H. Jin, X. Cai, S. Li, Y. Shen, Structural and mechanistic insights into the activation of Stromal interaction molecule 1 (STIM1), Proc. Natl. Acad. Sci. U. S. A. 109 (2012) 5657–5662, https://doi.org/10.1073/pnas.1118947109.
[28] P.B. Stathopulos, R. Schindl, M. Fahrner, L. Zheng, G.M. Gasmi-Seabrook, M. Muik, C. Romanin, M. Ikura, STIM1/Orai1 coiled-coil interplay in the regulation of store-operated calcium entry, Nat. Commun. 4 (2013) 2963, https://doi.org/10.1038/ncomms3963.
[29] V.C. Garside, A.S. Kowalik, C.L. Johnson, D. DiRenzo, S.F. Konieczny, C.L. Pin, MIST1 regulates the pancreatic acinar cell expression of Atp2c2, the gene encoding secretory pathway calcium ATPase 2, Exp. Cell Res. 316 (2010) 2859–2870. doi:https://doi.org/10.1016/j.yexcr.2010.06.014.
[30] Y. Sagara, G. Inesi, Inhibition of the sarcoplasmic reticulum Ca2+ transport ATPase by thapsigargin at subnanomolar concentrations, J. Biol. Chem. 266 (1991) 13503–13506.
[31] M.Y. Feng, R. Rao, New insights into store-independent Ca(2+) entry: secretory pathway calcium ATPase 2 in normal physiology and cancer, Int. J. Oral Sci. 5 (2013) 71–74, https://doi.org/10.1038/ijos.2013.23.
[32] H. He, M. Lam, T.S. McCormick, C.W. Distelhorst, Maintenance of calcium homeostasis in the endoplasmic reticulum by Bcl-2, J. Cell Biol. 138 (1997) 1219–1228, https://doi.org/10.1083/jcb.138.6.1219.
[33] S. Yamamoto, M. Takehara, Y. Kabashima, T. Fukutomi, M. Ushimaru, Identification of novel inhibitors of human SPCA2, Biochem. Biophys. Res. Commun. 477 (2016) 266–270, https://doi.org/10.1016/j.bbrc.2016.06.055.
[34] B.M. Cross, A. Hack, T.A. Reinhardt, R. Rao, SPCA2 regulates Orai1 trafficking and store independent Ca2+ entry in a model of lactation, PLoS One. 8 (2013) e67348. doi:https://doi.org/10.1371/journal.pone.0067348.
[35] S. Smaardijk, J. Chen, S. Kerselaers, T. Voets, J. Eggermont, P. Vangheluwe, Store-independent coupling between the secretory pathway Ca(2+) transport ATPase SPCA1 and Orai1 in Golgi stress and Hailey-Hailey disease, Biochim. Biophys. Acta. Mol. Cell Res. 1865 (2018) 855–862, https://doi.org/10.1016/j.bbamcr.2018.03.007.
[36] S. Smaardijk, J. Chen, F. Wuytack, P. Vangheluwe, SPCA2 couples Ca2+ influx via Orai1 to Ca2+ uptake into the Golgi/secretory pathway, Tissue Cell. 49 (2017) 141–149, https://doi.org/10.1016/j.tice.2016.09.004.
[37] V. Vigont, Y. Kolobkova, A. Skopin, O. Zimina, V. Zenin, L. Glushankova, E. Kaznacheyeva, Both Orai1 and TRPC1 are involved in excessive store-operated calcium entry in striatal neurons expressing mutant huntingtin exon 1., Front. Physiol. 6 (2015) 337. doi:https://doi.org/10.3389/fphys.2015.00337.
[38] J.H. Hong, Q. Li, M.S. Kim, D.M. Shin, S. Feske, L. Birnbaumer, K.T. Cheng, I.S. Ambudkar, S. Muallem, Polarized but differential localization and recruitment of STIM1, Orai1 and TRPC channels in secretory cells, Traffic. 12 (2011) 232–245, https://doi.org/10.1111/j.1600-0854.2010.01138.x.
[39] M.S. Kim, K.P. Lee, D. Yang, D.M. Shin, J. Abramowitz, S. Kiyonaka, L. Birnbaumer, Y. Mori, S. Muallem, Genetic and pharmacologic inhibition of the Ca2+ influx channel TRPC3 protects secretory epithelia from Ca2+-dependent toxicity., Gastroenterology. 140 (2011) 2107–15, 2115.e1–4. doi:https://doi.org/10.1053/j.gastro.2011.02.052.